

SPECIAL FEATURE

Price Prediction Based on
Time Series Analysis
with Ensemble Deep
Learning Models



Silicon University

The Science & Technology Magazine

Digital Digest

Vol. 33 • April - June 2025



Our Vision: "To become a center of excellence in the fields of
technical education & research and create responsible citizens"

The Rise of Robotic Process Automation: Redefining the Future of Work

In the era of digital transformation, Robotic Process Automation (RPA) has emerged as a transformative force, fundamentally altering company operations. Initially a mechanism for automating monotonous back-office functions, it has transformed into a strategic resource that boosts productivity, lowers expenses, and liberates human capacity for more valuable endeavours.

Robotic Process Automation employs software bots to replicate human activities within digital systems. These bots can access apps, input data, perform calculations, make rule-based choices, and initiate responses—all with a speed and precision that surpass human capabilities. RPA is optimizing operations, reducing errors, and ensuring consistent performance across several sectors, including finance and healthcare, continuously.

Still, RPA has worth beyond only efficiency. It resides in its capacity to enable people. RPA lets staff members concentrate on distinctive human qualities—creativity, problem-solving, and innovation—by absorbing routine and rule-based tasks. In a time when agility is more important than ever, companies with intelligent automation will be more suited to scale quickly and evolve.

Many times, critics of job displacement bring out issues. Although this worry is legitimate, history reveals that automation changes rather than replaces work. Leaders of today must reskill and upskill their employees to work with automation instead of vying against it. Companies that make investments in human capital alongside technology will find themselves on the side of the digital divide that benefits them.

Looking ahead, the combination of RPA with artificial intelligence and machine learning promises even more transforming power—cognitive bots that not only follow rules but also learn, analyse, and make difficult decisions. Often called Intelligent Automation, this new wave is rethinking what is feasible in many different sectors.

Robotic process automation is the pillar of the contemporary company, not only a trend. The issue now is not whether to use RPA but rather how quickly companies might expand it to produce long-term benefits. Work going forward is man with machine, not man against machine.

Dr. Pragyan Paramita Das

Dept. of CSE

Price Prediction Based on Time Series Analysis with Ensemble Deep Learning Models

Abstract—The high volatility and dynamic market behavior of cryptocurrency make it a significant challenge to predict their prices. The accuracy of both short-term and long-term price trend forecasts is improved by the integration of Temporal Convolutional Networks (TCN) and Convolutional Neural Networks (CNN) in an ensemble deep learning approach proposed in this study. The ensemble model effectively captures complex price movements by leveraging the spatial pattern recognition strengths of CNN and the temporal feature extraction capabilities of TCN. The proposed work outperforms numerous extant baseline models in terms of prediction accuracy and stability, as evidenced by experimental evaluations. This method offers traders, investors, and analysts valuable insights, facilitating more informed decision-making in the volatile cryptocurrency market.

Keywords—Cryptocurrency, CNN, TCN, Deep Learning, Bitcoin

I. Introduction

Satoshi Nakamoto created the digital currency Bitcoin in 2009. It employs blockchain technology, rendering each transaction publicly accessible. The price of Bitcoin experiences regular and rapid fluctuations. These changes may arise from new legislation, evolving public attitude, or technological improvements. This complicates the ability of conventional financial models to precisely predict its price. Individuals must understand both transient price variations and enduring trends to trade Bitcoin judiciously. Some investors target long-term growth, while others prefer immediate returns. Consequently, a predictive model that serves the interests of both categories of investors is necessary. Our aim is to create a model that delivers useful and precise predictions for diverse Bitcoin investment methods.

II. Literature Review

The application of deep learning has brought about a substantial shift in the field of financial forecasting, particularly in the prediction of the prices of cryptocurrencies and stocks. Traditional time series models, such as the AutoRegressive Integrated Moving Average (ARIMA) model [1], have been utilized for modeling and forecasting financial data for a considerable amount of time. This is due to the fact that these models are effective in capturing linear trends and temporal dependencies. On the other hand, ARIMA and other classical statistical models have demonstrated limitations in terms of their accuracy and flexibility in light of the arrival of big data as well as the growing complexity and non-linearity of financial markets.

In contrast, advanced deep learning models like as

Recurrent Neural Networks (RNN), Long Short-Term Memory (LSTM) networks, and Convolutional Neural Networks (CNN) have exhibited considerable performance gains. RNNs and LSTMs are well-suited for sequential data, capturing long-term dependencies and learning complicated temporal patterns across time, whilst ARIMA is focused on modeling historical price trends under the assumption of stationarity. On the other hand, ARIMA is primarily concerned with modeling historical price trends. Although CNNs have typically been utilized in the field of image processing, they have been successfully modified to deal with financial data in order to extract spatial or structural elements from sequences of prices, thereby improving their prediction accuracy [2].

The goal of increasing the accuracy of forecasting has led to the investigation of a wide range of models and methods, which have been investigated in a number of studies. For instance, Grieves (2018) [3] utilized logistic regression and Support Vector Machines (SVM) to forecast the direction in which prices would change. This provided the foundation for evaluating binary classification in the context of financial situations. In the meanwhile, Junwei Chen et al. [4] conducted research on a variety of machine learning models, such as decision trees and ensemble techniques. Their findings highlighted the predictive capability of non-linear algorithms when applied to price information.

A noteworthy method was presented by Chowdhury et al. [5], who created a hybrid model that included LSTM and RNN. This model enabled the network to take advantage of the sequential learning capabilities of RNNs as well as the memory-preserving capabilities of LSTMs. The utilization of this synergy proved to be successful in modeling extremely volatile

and noisy financial series, such as the prices of cryptocurrencies.

Lahmirmi and Bekiros [6] made an additional contribution to the body of research by contrasting a number of different LSTM architectures by employing performance metrics such as Mean Squared Error (MSE), Root Mean Squared Error (RMSE), Mean Absolute Error (MAE), and Mean Absolute Percentage Error (MAPE). The findings of their study revealed the durability of deep learning models, particularly when the hyperparameters were fine-tuned to achieve optimal effectiveness.

Kazeminia et al. [7] presented novel hybrid models that combine both conventional and deep learning strategies. This represents a significant advancement in the field. CNN-LSTM, which uses convolutional layers to extract features and LSTM layers for temporal analysis, was one of their models. Another model that they utilized was ARIMA-CNN-LSTM, which combines the capabilities of CNN-LSTM in capturing non-linear and complex structures with the capabilities of ARIMA in detecting linear trends. Through the utilization of this multi-stage modeling method, the model is able to first eliminate linear components by means of ARIMA, and then it is able to send the residuals to deep learning modules in order to capture detailed patterns within the data.

One conclusion that is clear across all of this research is that hybrid models have a tendency to perform better than traditional or deep learning models that are used on their own. Models that combine statistical methodologies with neural networks have been shown to achieve higher generalization and forecasting capacity, particularly in highly dynamic and unpredictable financial contexts [8]. These models have been evaluated using popular metrics like mean absolute error (MAE), root mean square error (RMSE), and accuracy levels.

Increasingly, there is a tendency toward merging the interpretability of statistical models with the representational capability of deep learning. This movement opens up intriguing paths for future study and practical applications in high-frequency trading, portfolio optimization, and algorithmic finance.

III. Proposed Methodology

The dataset utilized in this study is assembled from a variety of sources such as yfinance, Binance,

Cryptocompare and Alphavantage. It contains features such as open, high, low, close, prices, trading volume, dividends, and stock splits, and all are in USD.

To perform data preprocessing, it uses pandas to import datasets, performing exploratory data analysis (EDA), formatting dates, cleaning column names, eliminating features that weren't relevant, and dealing with missing values. To visualize relationships between variables, correlation matrices are used, which utilize seaborn. After merging and cleaning the final dataset exported it as a CSV file and divided it into an 80% training set and a 20% testing set. Before dividing the data set, we also scale our data to 0 to 1 using 'MinMaxScaler' shown in equation (1) where X_{MIN} & X_{MAX} are the lowest and highest values of the data set respectively.

$$X_{scaled} = \frac{X - X_{MIN}}{X_{MAX} - X_{MIN}} \quad (1)$$

ARIMA Model: Auto Regressive Integrated Moving Average (ARIMA) is a robust time series forecasting method widely employed for the analysis and prediction of univariate time series data. Comprising three key components, ARIMA models capture different aspects of temporal patterns. The ARIMA model is proficient at capturing past patterns by utilizing its autoregressive and moving average components. The three parameters that represent the lag observations, differencing, and moving average window size in the model are p (AR order), d (I order), and q (MA order), respectively.

Convolution Neural Network Model: Convolutional Neural Networks (CNNs) automatically learn complicated patterns from sequential data, so they are excellent at predicting cryptocurrency prices. CNNs use convolutional layers with filters to identify local patterns such as volatility and trends. In order to emphasize significant features, pooling layers down sample data and introduce non-linearity to model complex relationships. CNNs are capable of accurately projecting cryptocurrency data by identifying pertinent patterns in the data through the use of hierarchical feature extraction and adaptation to non-linear correlations. Additionally, resilient and scalable, CNNs are perfect for managing the large-scale datasets and the dynamic nature of the financial markets. In Equation (2), $S(i, j)$ is the output feature map, I is the input image, K is the kernel (filter), and denotes the convolution operation in CNN.

$$S(i, j) = (I \otimes K)(i, j) = \sum_m \sum_n I(i - m, j + n) * K(m, n) \quad (2)$$

Long Short-Term Memory Model: LSTM networks

can capture sequential correlations and long-range dependencies in time-series data, making them useful for predicting Bitcoin prices. They are ideal for volatile cryptocurrency markets since they are skilled at spotting trends, seasonality, and abnormalities in pricing data. The mean square error (MSE) metric was used to examine the performance of the experimental LSTM model with three layers and different activation functions like Rectified Linear Unit (ReLU), Tanh throughout multiple epochs (30, 50, and 100) in order to make adjustments for changing market conditions. The training process and performance of the model were visualized using learning curves.

CNN-LSTM Hybrid model: A hybrid model that combines an LSTM network and a convolutional neural network works well for predicting the price of Bitcoin. Using filters, the CNN collects short-term characteristics and local patterns from the input sequence to identify current trends and fluctuations. The CNN output is flattened and then reshaped to make it compatible with the LSTM layer. The LSTM layer is responsible for learning long-term dependencies and recognizing broad trends across several time steps. This hybrid model effectively captures a variety of temporal patterns in bitcoin price data by combining a CNN for short-term patterns and an LSTM for long-term. A final Dense layer produces the model's prediction, and training modifies the CNN and LSTM weights to maximize performance.

ARIMA-CNN-LSTM Hybrid model: This script builds an ensemble model for bitcoin value prediction by fusing traditional time series analysis (ARIMA) with deep learning techniques (CNN and LSTM). While ARIMA manages linear dependencies in the data, CNN and LSTM models capture non-linear patterns and temporal dependencies. While the CNN processes incoming data using a 1D convolutional layer, the LSTM integrates sequential information. Using residuals as the CNN-LSTM hybrid's input, the model improves ARIMA predictions while catching patterns that ARIMA was unable to identify. Various optimizers are examined, and RMSE measures are used to assess the model's performance. The ARIMA model is represented as:

$$Y_t = C + \phi_1 Y_{t-1} + \phi_2 Y_{t-2} + \dots + \phi_p Y_{t-p} + \theta_1 \epsilon_{t-1} + \theta_2 \epsilon_{t-2} + \dots + \theta_q \epsilon_{t-q} + \epsilon_t \quad (3)$$

Where Y_t is the value of the time series at time t , C is a constant term, $\phi_1, \phi_2, \dots, \phi_p$ are the autoregressive coefficients, ϵ_t is the white noise term at time t , $\theta_1, \theta_2, \dots$,

θ_q are the moving average coefficients.

For the CNN-LSTM hybrid model, r is defined as follows:

$$r = \sum_j \sum_k (W_{cnn} * X_{t+j-1,k} + b_{cnn}) \quad (4)$$

Where $X_{t+j-1,k} = Y_{t+j-1}$, assuming Y_t as the output of the ARIMA model.

The output Y_i of the CNN-LSTM hybrid model is obtained by:

$$Y_i = LSTM(Flatten(ReLU(r))) \quad (5)$$

The combined model integrates the ARIMA output Y_t into the CNN-LSTM model as an input sequence, represented as:

$$r = \sum_j \sum_k (W_{cnn} * X_{t+j-1,k} + \beta * Y_t + b_{cnn}) \quad (6)$$

And the final output Y_i is computed as:

$$Y_i = LSTM(Flatten(ReLU(r))) \quad (7)$$

Equation (6 & 7) shows how the CNN-LSTM model processes the sequence t to generate the final output Y_t . The ARIMA output Y_t serves as historical information to capture sequential dependencies and patterns in the time series data.

The ARIMA model is fitted to the given data, and forecasting is performed using the fitted ARIMA model to obtain predictions for the entire time series. Then we calculated the residual by subtracting the fitted values from the original time series, and scaled the residual using Min-Max scaling. The scaled residuals are used to create input-output pairs for the CNN-LSTM model. A Sequential model is created with layers including Conv1D, MaxPooling1D, LSTM, Dropout, and Dense layers. The model is compiled with a low learning rate using different optimizers and mean squared error loss. The trained model is used to make predictions on the training data.

RNN model: The capacity of recurrent neural networks (RNNs) to recognize patterns and sequential relationships across time makes them useful for predicting bitcoin prices. Recurrent connections enable RNNs to store memories of previous data, which enables them to learn from historical price sequences and anticipate future events based on patterns and temporal relationships in the data. For the analysis of time-series data, such as bitcoin prices, where past values can affect future movements, RNNs are ideally suited.

GRU model: Like LSTMs, Gated Recurrent Units (GRUs) can capture long-range dependencies in sequential data while minimizing problems like vanishing gradients, which makes them useful for predicting cryptocurrency prices. Because GRUs are so good at remembering details over extended periods of time, they are perfect for examining temporal patterns and trends in data on bitcoin prices. Because of their less complicated construction than LSTMs, they are computationally efficient, which is useful for accurately modeling intricate financial time series. All things considered, GRUs provide a dependable and successful method for evaluating sequential data and forecasting Bitcoin values.

TCN model: Because dilated convolutions allow temporal convolutional networks (TCNs) to capture long-range relationships in time-series data, TCNs are useful for predicting the price of Bitcoin. Because of this feature, TCNs may simulate intricate and dynamic patterns in bitcoin values without the need for recurrent connections like RNNs, including short-term oscillations and longer-term trends. Because of their parallel processing capabilities, TCNs are scalable and effective for managing massive financial datasets. This makes them a great foundation for precise and adaptable bitcoin price prediction based on temporal patterns that have been learned.

TCN-RNN model: To effectively predict bitcoin values, the hybrid TCN-RNN model blends Temporal Convolutional Networks (TCNs) with Recurrent Neural Networks (RNNs). Convolutional operations with different dilation rates are used by TCN layers with causal padding to capture a variety of time-scale patterns. An RNN layer receives the output from TCN layers to handle long-term linkages and sequential dependencies. In order to forecast bitcoin prices based on past trends and reduce loss (such as mean squared error), the model is trained using gradient-based optimization. Mean Absolute Error (MAE) and other evaluation measures show how flexible and dependable this hybrid model is for financial time-series forecasting.

TCN-LSTM model: For predicting Bitcoin prices, a hybrid model that combines Long Short-Term Memory (LSTM) networks with Temporal Convolutional Networks (TCNs) works well. While LSTM layers reflect long-term dependencies and sequential interactions, TCN layers use variable dilation rates to capture short-term properties. Using weight adjustments to get precise predictions, the

model is trained to minimize a loss function such as mean squared error. The final forecast is produced by a Dense layer, and measures such as Mean Absolute Error (MAE) are used to evaluate its success. This method effectively addresses both long-term trends and short-term volatility in financial data by utilizing TCNs and LSTMs to uncover intricate patterns.

TCN-GRU model: The hybrid model that combines Gated Recurrent Units (GRUs) and Temporal Convolutional Networks (TCNs) efficiently captures both long-term dependencies and short-term volatility in cryptocurrency price data. While TCNs are excellent at extracting local patterns, GRUs learn sequential connections over several time steps. The model is flexible and effective for time-series forecasting in financial markets since it is trained using gradient-based optimization (such as the Adam optimizer) to minimize loss.

Integrated Temporal and Convolutional Network (ITCN): Convolutional neural networks (CNNs) and temporal convolutional networks (TCNs) combined provide a powerful framework for predicting and evaluating time-series data, such as cryptocurrency values. Because of this hybrid design, which combines CNNs' feature extraction skills with TCNs' strengths in capturing hierarchical connections, the model can extract both global and local characteristics from the input. Sequential and convolutional layers that have been tuned for time-series analysis are utilized by the TCN-CNN hybrid model as shown in Fig. 1. The TCN component captures various temporal scales and patterns by using dilated convolutional layers with varied dilation rates. A CNN block that uses batch normalization and max-pooling techniques to further process the extracted features comes after these layers.

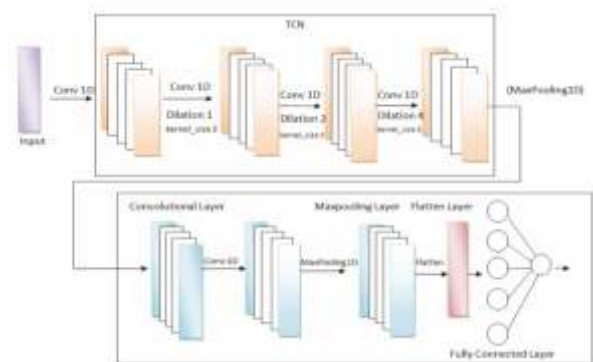


Fig. 1 ITCN Architecture for Cryptocurrency Price Prediction

For the final prediction, the CNN block's output is flattened and run through several thick layers. While the CNN layers are excellent at extracting significant features and global patterns, the TCN layers are in charge of capturing local temporal dependencies and feature hierarchies within the data. The hybrid model successfully combines local and global data to anticipate bitcoin price patterns by blending these two designs. The output $x_i^{(l)}$ at layer l and time step i is computed using a dilated convolution operation:

$$x_i^{(l)} = f(\sum_{j=0}^{k-1} w_j^{(l)} * x_{i-dj}^{(l-1)} + b^{(l)}) \quad (8)$$

Here, f is the activation function applied element-wise (e.g., ReLU), $w_j^{(l)}$ are the weights of the convolutional filter, d is the dilation rate, k is the kernel size, and b is the bias term.

The hybrid model is trained to minimize a given loss function (such as mean squared error) using gradient-based optimization techniques. As a regularization strategy, early halting is used to reduce overfitting and enhance generalization. Metrics like Mean Absolute Error (MAE) are used to analyze the performance of the model in order to determine how accurate and dependable it is at predicting cryptocurrency values. A versatile framework for time-series forecasting in financial markets is offered by the TCN-CNN hybrid model. The model is appropriate for real-time prediction problems since it integrates CNNs and TCNs to capture dynamic information and complex temporal patterns.

IV. Results and Observations

We evaluated the performance of our models using the performance metric Akaike Information Criterion (AIC), Mean Squared Error (MSE), Accuracy, and Error percentage.

From Table 1, we observe that the performance of the model with parameters (7,1,5) is good as indicated by its low AIC (42501.49) and relatively low RMSE (13480.02), suggesting a good balance between model fit and accuracy in predicting cryptocurrency prices.

Table-1: Results of ARIMA

Parameters	AIC	RMSE
(6,1,5)	42501.854	13319.615
(7,1,9)	41501.036	18310.414
(9,1,8)	42448.262	13809.559
(4,1,5)	42484.346	14053.046
(7,1,5)	42501.491	13480.017
(5,1,5)	42470.686	13778.386

Other models like (9,1,8) also show competitive AIC values, indicating potential effectiveness in forecasting, though specific performance metrics may vary.

From Table 2, we observe that Stochastic Gradient Descent (SGD) with ReLU activation and MSE loss achieved the highest accuracy (93.57%). ReLU consistently outperformed Tanh across all optimizers.

Table-2: Results of CNN

Optimizer	Activation	Loss Function	Accuracy	Error
RmsProp	relu	MSE	84.80%	15.20%
RmsProp	tanh	MSE	79.21%	20.79%
Adam	relu	MSE	77.53%	22.47%
Adam	tanh	MSE	75.20%	24.80%
SGD	relu	MSE	93.57%	6.43%
SGD	tanh	MSE	82.41%	17.59%

From Table 3, it can be observed that using the Adam optimizer, the model peaked at 91.54% accuracy at 50 epochs but dropped to 83.27% by 100 epochs. Root Mean Squared Propagation (RmsProp) declined from 83.51% at 50 epochs to 80.90% at 30 epochs. SGD showed consistent performance, improving marginally from 84.92% at 30 epochs to 84.58% at 100 epochs. RmsProp was stable, while SGD consistently improved with more epochs.

Table-3. Results of LSTM

Optimizer	Epochs	Loss Function	Accuracy	Error (%)
Adam	50	MSE	91.54%	8.46%
Adam	100	MSE	83.27%	16.73%
RmsProp	50	MSE	83.51%	16.49%
RmsProp	30	MSE	80.90%	19.10%
SGD	100	MSE	84.58%	15.42%
SGD	30	MSE	84.92%	15.08%

The CNN-LSTM ensemble uses a 0.2 dropout rate to prevent overfitting and includes an LSTM with 50 neurons for long-term pattern recognition. Different optimizers and activation functions were tested during compilation. Historical data from various platforms was used for training over 50–100 epochs, evaluating performance with Mean Absolute Error (MAE) and optimizing using Mean Squared Error (MSE) loss. Table 4 shows that the Adam optimizer consistently outperforms Rmsprop across all configurations in optimizing the Ensemble model. Adam paired with ReLU activation achieves the highest accuracy of 92.14%, showcasing superior convergence and predictive capability. ReLU consistently performs tanh activation regardless of the optimizer used. The

Table-4. Result of CNN-LSTM Hybrid Model

Optimizer	Activation	Loss Function	Accuracy	Error
Adam	ReLU	MSE	92.14%	7.86%
Adam	tanh	MSE	87.90%	12.10%
RmsProp	ReLU	MSE	84.95%	15.07%
RmsProp	tanh	MSE	86.51%	13.49%

synergy of Adam optimizer, ReLU activation, and MSE loss leads to an impressive accuracy of 92.14%, highlighting the importance of activation functions in improving the model's ability to identify complex patterns in cryptocurrency price fluctuations.

From Table 5, we can observe that there's minimal difference in performance among the Adam, Rmsprop, and SGD optimizers, suggesting that optimizer choice has a limited impact on RMSE. Activation functions (relu vs. tanh) for CNN and LSTM layers do not consistently influence model performance. A configuration using the SGD optimizer with "ReLU" activation for CNN and LSTM layers achieved the lowest RMSE of 15980.04. Overall, RMSE values are relatively close across configurations, indicating consistent but not sig- significantly different model performance with varied optimizer, activation, and loss function choices.

Table-5. Result of ARIMA-CNN-LSTM

Optimizer	Activation (CNN)	Loss Function	RMSE
Adam	ReLU	MSE	16014.94
Adam	tanh	MSE	
Adam	ReLU	MSE	16014.22
Adam	ReLU	MSE	16014.27
Adam	tanh	MSE	16014.99
RmsProp	ReLU	MSE	16015.01
RmsProp	tanh	MSE	
RmsProp	ReLU	MSE	16014.44
RmsProp	ReLU	MSE	16014.59
RmsProp	tanh	MSE	16015.10
SGD	ReLU	MSE	16000.36
SGD	tanh	MSE	
SGD	ReLU	MSE	15980.04
SGD	tanh	MSE	16003.80

Table 6, we can observe that the Adam optimizer consistently achieved the lowest test mean absolute error (MAE) and test loss values across different configurations, with a notable MAE of 0.000003 and

Table-6: Result of TCN

Optimizer	Activation	Loss Function	Test MAE	Test Loss
RmsProp	ReLU	MAE	0.00387	0.00487
RmsProp	Tanh	MAE	0.00155	0.01060
RmsProp	Sigmoid	MAE	0.00958	0.03005
Adam	ReLU	MAE	0.00036	0.00069
Adam	Tanh	MAE	0.00259	0.00351
Adam	Sigmoid	MAE	0.00535	0.00457
SGD	ReLU	MAE	0.00065	0.00512
SGD	Tanh	MAE	0.00118	0.00391
SGD	Sigmoid	MAE	0.00298	0.21559

test loss of 0.000985 using Relu activation. In contrast, SGD with Sigmoid activation performed less effectively with higher MAE and loss.

These findings underscore the importance of selecting optimal optimization strategies and activation functions to maximize model accuracy in cryptocurrency price prediction tasks, highlighting the resilience and efficiency of the Adam optimizer.

From Table 7, we can observe that the TCN-LSTM hybrid model's prediction accuracy, measured by MAE, was notably better (0.17278) when using Relu for the TCN layer and Sigmoid for the LSTM layer with the Adam optimizer. Activation function configurations and optimizers (RmsProp, Adam, SGD) significantly impacted model performance, with Adam consistently outperforming others. Fine-tuning hyperparameters is crucial for optimizing model performance in cryptocurrency price forecasting tasks, suggesting avenues for further improvement and robustness.

Table-7. Result of TCN-LSTM

Optimizer	Activation (TCN)	Activation (LSTM)	Test MAE	Test Loss
RmsProp	ReLU	ReLU	0.17268	0.04505
	Tanh	Sigmoid ReLU	0.17272	0.04507
	Sigmoid		0.17269	0.04506
Adam	ReLU	ReLU	0.17265	0.04505
	ReLU	Sigmoid ReLU	0.17272	0.04507
	Sigmoid		0.17278	0.04511
SGD	ReLU	ReLU	0.17272	0.04507
	Tanh	ReLU	0.17269	0.04506
	Sigmoid	Tanh	0.17304	0.04530

We can observe from Table-8 that the TCN-GRU hybrid model's performance in cryptocurrency price prediction is strongly influenced by optimizer and activation function choices. The Adam optimizer consistently produced lower test MAE values across various configurations. The best performance (MAE of 0.17222, loss of 0.04517) was achieved with Relu activation for TCN and Sigmoid activation for GRU layers. Overall, the Adam optimizer proved most effective for optimizing the TCN-GRU model in bitcoin price prediction tasks.

Table-8. Result of TCN-GRU

Optimizer	Activation (TCN)	Activation (GRU)	Test MAE	Test Loss
RmsProp	ReLU	ReLU	0.17254	0.04516
	Tanh Sigmoid	Sigmoid ReLU	0.17273	0.04506
			0.17258	0.04517
Adam	ReLU	ReLU	0.17242	0.04537
	ReLU	Sigmoid ReLU	0.17222	0.04517
	Sigmoid		0.17257	0.04512
SGD	ReLU	ReLU	0.17275	0.04504
	Tanh Sigmoid	ReLU	0.17281	0.04508
		Tanh	0.17267	0.04502

We can observe from Table 9 that RmsProp with ReLU activation consistently achieves the lowest

mean absolute error (MAE) and test loss values compared to Adam and SGD for TCN configurations. Tanh activation performs competitively but with slightly higher MAE and test loss. Sigmoid activation generally yields poorer results. The choice of optimizer and activation function significantly influences model performance, highlighting RmsProp with ReLU activation as a promising configuration for accurate cryptocurrency price prediction. Table 10 shows how different optimizer and activation function combinations affect the model's performance. When compared to RmsProp and SGD, employing the Adam optimizer consistently resulted in reduced test mean absolute error (MAE) and test loss values across a range of configurations. In particular, comparatively low MAE and loss values were obtained when the Adam optimizer with Relu activation was used for both the CNN and TCN layers, showing improved predictive accuracy. Notably, the lowest test MAE of 0.00411 and test loss of 0.00029 were obtained with the use of the Adam optimizer in conjunction with Sigmoid activation for the TCN layer and Relu activation for the CNN layer. This indicates potential performance in tasks involving the prediction of cryptocurrency prices.

Table-9. Result of TCN-RNN

Optimizer	Activation (TCN)	Activation (RNN)	Test MAE	Test Loss
RmsProp	ReLU	-	0.00249	1.18×10^{-5}
	Tanh	ReLU	0.00548	3.87×10^{-5}
	Sigmoid	-	0.18053	0.04861
Adam	ReLU	-	0.00480	3.52×10^{-6}
	ReLU	Sigmoid	0.00136	4.41×10^{-6}
	Sigmoid	-	0.00143	4.04×10^{-6}
SGD	ReLU	-	0.00132	6.00×10^{-6}
	Tanh	-	0.00128	5.76×10^{-6}
	Sigmoid	Tanh	0.18056	0.04850

Table-10. Result of ITCN

Optimizer	Activation (TCN)	Activation (CNN)	Test MAE	Test Loss
RmsProp	ReLU	ReLU	0.00872	0.00011
	Tanh	ReLU	0.01068	0.00029
	Sigmoid	ReLU	0.01036	0.00016
Adam	ReLU	ReLU	0.00567	0.00055
	ReLU	Sigmoid	0.01835	0.00056
	Sigmoid	ReLU	0.00411	0.00029
SGD	ReLU	ReLU	0.00614	0.00055
	Tanh	ReLU	0.00909	0.00099
	Sigmoid	Tanh	0.01375	0.00030

Important insights on model performance and optimization techniques are revealed by analyzing the experimental results obtained from several models for predicting the price of cryptocurrencies. The accuracy

and model fit of the ARIMA model were balanced, with the (7,1,5) parameterization obtaining the lowest AIC and comparatively low RMSE. The CNN model had a high accuracy of 93.57% when using SGD with ReLU activation in deep learning models, but the LSTM model with Adam optimizer at 50 epochs achieved the greatest accuracy of 91.54%. Under the Adam optimizer, hybrid models like CNN-LSTM and TCN-LSTM showed increased accuracy when using particular activation functions (like ReLU for TCN). The TCN model demonstrated remarkable performance when paired with the Adam optimizer with ReLU activation, yielding the lowest test MAE and loss values. Moreover, our proposed model, Integrated Temporal and Convolutional Network (ITCN), proved to be highly accurate in datasets of different sizes, proving its usefulness in situations involving both small and big amounts of data. When compared to alternative architectures, the ITCN model, which was optimized using the Adam optimizer and the ReLU activation function, continuously showed the highest accuracy with the lowest mean absolute error (MAE) and loss values.

V. Conclusion

Our study compared several models for cryptocurrency price prediction, including ARIMA, CNN, LSTM, GRU, RNN, TCN, and hybrid architectures like CNN-LSTM, ARIMA-CNN-LSTM, TCN-LSTM, TCN-GRU, TCN-RNN, and our proposed model, ITCN. Although the accuracy and performance of each model varied, our suggested model, i.e., ITCN, proved to be the most successful approach. In terms of accuracy and resilience, the ITCN model outperformed other architectures, demonstrating steady performance throughout a range of dataset sizes. With minimal mean squared error and mean absolute error, we obtained greater accuracy, in contrast to several other models that provided competitive results but had limits in terms of scalability or complexity.

Acknowledgment

We wish to express our gratitude to Prof. Milan Samantaray of the Department of Computer Science & Engineering at Silicon University for her generous support and advice.

References

- [1] I. M. Wirawan, T. Widiyaningtyas, and M. M. Hasan, Short Term Prediction on Bitcoin Price Using ARIMA Method, in IEEE, 2019. DOI: 10.1109/isemantic.2019.8884257.
- [2] E. Sin and L. Wang, Bitcoin Price Prediction Using Ensembles of Neural Networks, in 2017 13th International Conference on Natural Computation, Fuzzy Systems and Knowledge Discovery (ICNC-FSKD), IEEE, 2017, pp. 666–671.
- [3] I. E. Livieris, N. Kiriakidou, S. Stavroyiannis, and P. Pintelas, An Advanced CNN-LSTM Model for Cryptocurrency Forecasting, Electronics (Basel), vol. 10, no. 3, p. 287, 2023. DOI: 10.3390/electronics10030287.
- [4] O. Snihovyi, O. Ivanov, and V. Kobets, Cryptocurrencies Prices Forecasting with Anaconda Tool Using Machine Learning Techniques, in CEUR Workshop Proceedings, vol. 2105, 2018, pp. 453–456.
- [5] R. Chowdhury, M. A. Rahman, M. S. Rahman, and M. R. C. Mahdy, An Approach to Predict and Forecast the Price of Constituents and Index of Cryptocurrency Using Machine Learning, Physica A: Statistical Mechanics and its Applications, vol. 551, p. 124569, 2020. DOI: 10.1016/j.physa.2019.124569.
- [6] S. Lahmiri and S. Bekiros, Cryptocurrency Forecasting with Deep Learning Chaotic Neural Networks, Chaos, Solitons & Fractals, vol. 118, pp. 35–40, 2019.
- [7] S. Kazemina, H. Sajedi, and M. Arjmand, Real-Time Bitcoin Price Prediction Using Ensemble 2D-CNN LSTM Model, in IEEE, 2023. DOI: 10.1109/icwr57742.2023.10139275.
- [8] B. P. Kolla, Predicting Crypto Currency Prices Using Machine Learning and Deep Learning Techniques, International Journal of Advanced

**Ananya Nayak, Rajashree Senapati,
Saswat Tripathy**
M. Sc. (Data Science)

Some unbreakable encryption keys are accidentally leaking online

A widely used form of encryption called RSA (Rivest-Shamir-Adleman) is thought to be unbreakable, but an analysis of more than 5 billion server records has found that, in some cases, hardware errors can lead to secret keys being exposed.

Hardware faults are leaking hundreds of supposedly unbreakable encryption keys onto the internet, researchers have found – and spy agencies may be exploiting the loophole to read secret messages.

RSA is a widely-used encryption scheme that depends on two numbers – a public key, which anyone can use to encrypt a message intended for a particular person, and a private key, which decrypts the messages and only that person has access to it. Individuals can also use their private key to “sign” a message, allowing anyone to use their public key. Encryption is essential for data security, but faulty encryption can do more harm than good. Weak algorithms, poor key management, and implementation flaws can expose sensitive information to cyber threats.

Here's how to ensure your encryption is solid: Use

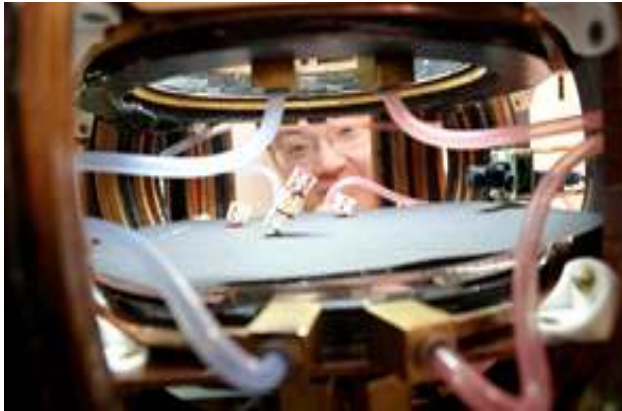


modern, strong encryption standards (AES-256, RSA-4096, ECC). Secure encryption keys in a vault, not in code. Keep TLS (Transport Layer Security) updated to protect data in transit. Regularly audit and test encryption practices.

It reinforces the importance of proper encryption and encourages immediate action.

Source: www.newscientist.com

Metabot



A metabot is a metamaterial with the ability to move and change shape. Princeton University has created a metabot that can expand, change shape, move, and respond to electromagnetic commands like a remotely controlled robot. The researchers dubbed sequences from the Transformers film. The electromagnetic fields carry both Power and signal simultaneously. Although each activity is quite basic, when combined, they can exhibit a great deal of complexity. This study shows that complex robotic motions can be triggered by passing torque over a distance remotely. The metabot consists of a modular collection of several mirror-image reconfigurable unit cells. A single push can cause the metabot to undergo significant morphing, including twisting, contracting, and shrinking. The complex behaviour is made possible by mirroring, which is known as chirality.

Source: SciTech Daily

Quantum Networking Chip

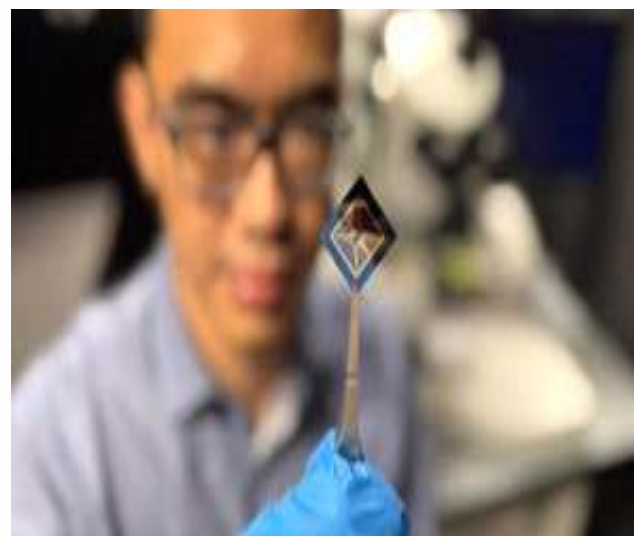
Cisco Systems demonstrated a prototype chip for the networking of quantum computers. The chip would assist in connecting smaller quantum computers into bigger systems and shares some of the same technologies as existing networking chips. Initially, the chip will be used in assisting scientists in detecting meteorites or financial organizations in synchronizing trading timing. In recent months, Nvidia intends to establish its quantum computing center, and Alphabet's Google, Microsoft, and Amazon have all revealed quantum computing chips. Additionally, PsiQuantum and other startups are raising hundreds of millions of dollars to develop systems.

Source: Indian Express



Vulcan, Amazon's Latest Robot

At Amazon's "Delivering the Future" event in Dortmund, Germany, a new robot was introduced, called the Vulcan robot. It represents a "fundamental leap in robotics." It is a touch-sensitive robot that can grasp and raise a variety of objects in its warehouse. This robot has been built to help humans with activities like selecting goods for storage and getting them ready for delivery. It is set to be deployed globally in the coming years. Robots have so far achieved some amazing feats, including driving automobiles, cleaning and ironing, and defeating



humans in chess masters, among other tasks. The sense of touch has remained absent from robotics, despite advancements in physical agility.

Source: Indian Express

Tiny Chip Sees Like an Eye

RMIT University engineers have developed a small, brain-like gadget that can process information, store visual memories, and recognize hand gestures without the need for an external computer. This is a neuromorphic device, which simulates the functioning of the human brain. Neuromorphic vision technology integrates visual tasks by employing analog-style processing, in contrast to digital systems



that use a lot of energy. So it has higher energy efficiency. The core of the system is compound metal Molybdenum disulfide (MoS₂). The minuscule atomic flaws of the metal can detect Light and transform into electrical signals. The gadget can record and process visual data in real time since this is comparable to how neurons fire and communicate in the brain.

Source: SciTech Daily

Whoop 5.0

The Whoop 5.0 and Whoop MG, two new gadgets from the US-based health tech and wearables company Whoop, are brimming with health features, including hormone insights, heart screener with ECG, blood pressure insights, and more. The devices have a battery life of over 14 days and are 7% smaller than the Whoop 4.0 band. This is a complete reinvention of the WHOOP experience. With this launch, WHOOP enters a new health platform that gives people the ability to regain control over their health at a time when healthcare systems are reactive and frequently unavailable. WHOOP is going to be a primary health operating system. In India, Whoop bands cost about the same as Samsung and Google smart watches. However, because they are supposed to provide



precise fitness measurements, they are especially well-liked by sportsmen. Football player Cristiano Ronaldo is an investor and global spokesperson for the tech business.

Source: Indian Express

Train AI at Light Speed

Neural networks—software that simulates biological neural tissue—are the foundation of most AI systems. Neural networks connect layers of basic components, or "nodes," to enable AI systems to carry out complicated tasks, just like neurons connect to enable biological beings to think. These nodes only "fire" when a threshold is achieved in both artificial and biological systems; this is a nonlinear process that enables little input changes to result in more significant and intricate output modifications. Adding layers has little effect without such nonlinearity; instead, the system devolves into a single-layer linear operation in which inputs are merely joined together without any actual learning taking place. But none have solved the challenge of representing nonlinear functions using only light — until now. The first programmable chip that can use light to train nonlinear neural networks has been created by Penn engineers. This huge advancement might greatly speed up AI training, reduce energy usage, and possibly pave the way for completely light-powered computing systems. This new device is photonic, meaning it uses light beams to execute calculations, in contrast to traditional AI computers that run on electricity. The study, which was published in Nature Photonics, shows how the chip uses light manipulation to carry out the intricate nonlinear operations necessary for contemporary artificial intelligence.

Source: SciTech Daily

Dr. Chittaranjan Mohapatra
Dept. of CSE

IoT-Based Smart Disaster Management System

Abstract—Disasters such as earthquakes, floods, and fires pose serious threats to human life and infrastructure. Traditional disaster response systems often depend on manual intervention, which can be slow and inefficient. This work presents an IoT-based smart Disaster Management System that uses a network of sensors and microcontrollers to monitor environmental parameters in real-time. Parameters like temperature, humidity, gas concentration, water levels, and seismic activity are continuously monitored. Upon detecting anomalies, the system alerts users and authorities through buzzer alarms, displays, or potentially mobile alerts. This solution is low-cost, scalable, and suitable for both urban and remote deployments, thereby enhancing public safety and disaster preparedness.

Keywords—Internet of Things (IoT), Disaster Management, Sensor Networks, Real-time Monitoring

I. Introduction

Disasters such as floods, earthquakes, and fires continue to pose severe threats to human life, infrastructure, and the environment. Traditional disaster management systems often rely on manual processes, which can delay response times and limit effectiveness during critical events. In response to this challenge, this study presents an IoT-based smart disaster management system that leverages real-time environmental monitoring through embedded systems. The proposed system integrates soil moisture sensors for flood detection, flame sensors for fire detection, and vibration sensors (SW-420) for earthquake detection, all connected to an Arduino Nano microcontroller that serves as the system's control unit. These sensors continuously monitor their respective environmental parameters and send real-time data to the microcontroller. If a hazard is detected based on predefined thresholds, the system immediately activates an audible buzzer and displays a corresponding warning message on an Organic Light Emitting Diode (OLED) screen, alerting nearby individuals. The system is designed to reset automatically after each alert, enabling continuous and uninterrupted operation. Due to its low power consumption, minimal cost, and compact design, this system is ideal for deployment in homes, schools, community centers, and small industrial or rural setups where advanced disaster management infrastructure may not be available. Additionally, the modular nature of the system allows for future integration with components like Global System for Mobile Communications (GSM), and Global

Positioning System (GPS) modules for remote alerting and location tracking. This work demonstrates the effectiveness of using IoT and embedded technologies in real-time disaster monitoring and alert systems. By minimizing human intervention and enabling early detection, the system can significantly improve disaster preparedness and response, ultimately contributing to safer and more resilient communities.

The integration of IoT in disaster management systems has enabled more accurate monitoring, faster decision-making, and effective emergency responses. IoT-based systems leverage a network of interconnected sensors, communication devices, and cloud platforms to detect and respond to natural disasters in real time. For example, Kumar et al. [1] developed an IoT-based flood detection system using ultrasonic sensors to monitor water levels and alert authorities through SMS. Patil and Kale [2] proposed a wildfire monitoring framework using temperature, humidity, and gas sensors that can trigger alerts via GSM modules to reduce human loss and damage.

Advanced IoT frameworks often include edge computing and cloud integration to ensure real-time data processing and accessibility even in remote or disaster-prone areas [3]. Sharma et al. [4] emphasized the role of machine learning with IoT for predictive analysis in earthquake detection, improving both early warning accuracy and post-disaster resource allocation. However, key challenges such as sensor accuracy, energy efficiency, and data privacy still hinder large-scale deployment in all regions [5].

II. Proposed Method

System Overview:

The system utilizes multiple environmental sensors interfaced with an Arduino Nano microcontroller. Data from soil moisture, flame, and vibration sensors is processed to detect hazardous conditions. Alerts are displayed on an OLED screen and are sounded via a buzzer.

Soil Moisture Sensor: Detects high water content, indicating flooding

Flame Sensor: Detects the presence of fire

SW-420 Vibration Sensor: Identifies seismic activity

Sensing Domain

The sensors continuously monitor their respective environments. Each sensor has threshold values configured in the microcontroller. When a threshold is breached, a corresponding alert is triggered.

Control Domain

The Arduino Nano processes sensor data and makes decisions based on pre-defined logic. If a specific condition is met, such as moisture exceeding safe levels or seismic vibrations being detected, the system activates alerts.

Output Domain

Upon detecting danger, the system sounds a buzzer for 5 seconds and displays a message on OLED based on the type of hazard (e.g., "Earthquake Danger", "Fire Danger", "Water Level Increasing")

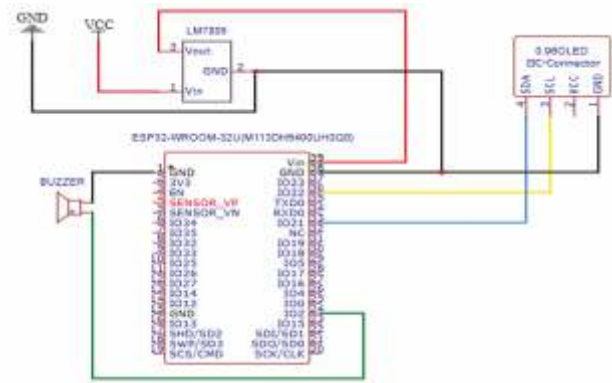
Components Used :

- ESP-32 WIFI MODULE
- Soil Moisture Sensor
- SW-420 Vibration Sensor
- Flame Sensor
- OLED Display
- Buzzer
- 12V Adapter
- LM7805 Voltage Regulator

III. System Architecture

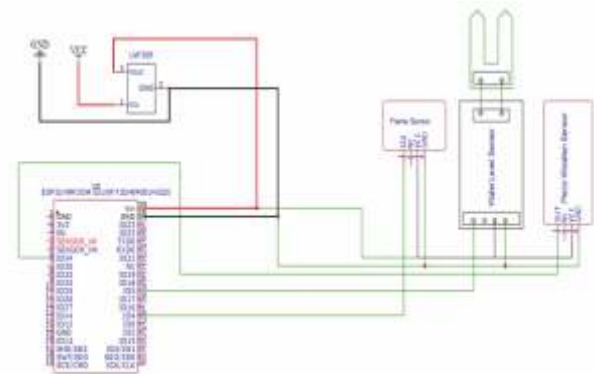
The proposed IoT-Based Smart Disaster Management System operates through the integration of multiple

environmental sensors connected to an Arduino Nano microcontroller, as shown in Figures 1 and 2. Upon powering the system, it initializes all sensors and output devices, including the OLED display and buzzer. The sensors involved in the system are the soil moisture sensor, flame sensor, and SW-420 vibration sensor, each responsible for detecting a specific type of disaster. These sensors continuously monitor their respective environmental parameters and send real-time data to the Arduino Nano, which serves as the system's control unit.



Receiver Circuit Module

Fig. 1. Proposed System Architecture



Transmitter Circuit Module

Fig. 2. The Output module

The soil moisture sensor is used to detect water levels in the ground, making it an essential component for flood detection. When the sensor senses moisture beyond a predefined threshold, the system interprets it as a potential flooding situation and activates the alert mechanism. Similarly, the flame sensor detects infrared radiation, and when the sensor output falls below a certain level, it signals the presence of fire. For earthquake detection, the SW-420 vibration sensor measures vibrations or shock waves, and if the measured values exceed the set threshold, the system assumes seismic activity.

Once a hazardous condition is detected by any sensor, the Arduino processes the data and triggers appropriate alerts. A buzzer is activated for five seconds to provide an audible warning, while the OLED display shows a message specific to the type of disaster, such as “Earthquake Danger,” “Fire Danger,” or “Water Level Increasing.” After issuing the alert, the system automatically resets itself and continues monitoring the environment without any manual intervention. This ensures that the system remains active and responsive to further threats.

The system's real-time response capability, coupled with its modular and low-power design, makes it highly suitable for small-scale implementation in homes, schools, and public buildings. It operates independently, requires minimal maintenance, and can be enhanced with additional sensors or communication modules for wider applicability. Overall, the system demonstrates a reliable and effective approach to early disaster detection and alerting using IoT technology.

IV. Results and Performance Analysis

The IoT-Based Smart Disaster Management System was rigorously tested under various simulated conditions to evaluate its accuracy, reliability, and real-time responsiveness. The primary objective of testing was to ensure that each sensor accurately detected its respective environmental parameter and that the system responded promptly with appropriate alerts. The testing procedure began with hardware validation, ensuring all sensors—soil moisture, flame, and vibration—were correctly connected to the Arduino Nano and powered appropriately. Once the system was powered on, it was observed for proper initialization of the OLED display and buzzer without triggering any false alerts.

To simulate a flood-like condition, water was gradually introduced around the soil moisture sensor. When the moisture level exceeded the predefined threshold, the system successfully displayed “Water Level Increasing” on the OLED and activated the buzzer for five seconds, confirming proper flood detection. Fire hazard simulation involved bringing a flame source close to the flame sensor. The sensor accurately detected the infrared radiation and triggered the “Fire Danger” alert on the display alongside the buzzer. Similarly, an earthquake simulation was conducted by creating controlled

vibrations near the SW-420 sensor. The system responded by displaying “Earthquake Danger” and sounding the buzzer, validating the effectiveness of vibration-based detection.

Response time across all scenarios was consistently under one second, which demonstrates the system's capability to provide immediate warnings. The system successfully reset after each alert and resumed monitoring, indicating stable and continuous operation without requiring manual intervention. Long-duration tests were also performed to assess the reliability of the system over extended periods. The system operated without any false positives or sensor drift, confirming its robustness and low power consumption.

Overall, the testing outcomes revealed that the system performed efficiently under different environmental conditions, with high accuracy and a low error margin. The integration of simple, low-cost components with an effective control algorithm resulted in a practical and scalable disaster alert system. These results validate the system's suitability for real-world deployment in homes, schools, industrial zones, and public buildings, especially in areas prone to natural disasters.

Applications:

1. **Urban Disaster Monitoring:** The system can be deployed in urban areas to monitor early signs of earthquakes, fires, or floods, especially in high-density zones where rapid response is critical.
2. **Remote and Rural Areas:** In regions lacking access to advanced monitoring infrastructure, this low-cost system offers a reliable alternative for early disaster detection and response.
3. **Educational Institutions and Public Buildings:** The system can be installed in schools, hospitals, and offices to enhance safety protocols and provide immediate alerts in case of environmental hazards.
4. **Smart Homes and Community Centers:** For personal or community-based disaster preparedness, the system can act as an always-on alert mechanism to protect life and property.
5. **Industrial and Hazard-Prone Zones:** The system can monitor environmental parameters in factories, chemical plants, or flood-prone zones to preemptively detect risks and reduce the impact of disasters.

6. Emergency Response Systems: When integrated with GSM or GPS modules, it can assist in emergency alert transmission to authorities or rescue teams for faster response.

V. Conclusions

The IoT-based smart disaster management system developed in this study successfully demonstrates how modern embedded technologies and low-cost sensors can be utilized to create an effective and reliable early warning system for natural disasters such as floods, fires, and earthquakes. By integrating soil moisture, flame, and vibration sensors with an Arduino Nano microcontroller, the system is capable of real-time monitoring of environmental parameters and immediate hazard detection. When a potential threat is identified based on predefined threshold values, the system activates a buzzer and displays an alert message on an OLED screen, ensuring that individuals in the vicinity are quickly informed of the danger. One of the key strengths of this system is its ability to reset automatically and resume continuous monitoring without manual intervention, making it a practical solution for round-the-clock disaster surveillance. The design emphasizes affordability, simplicity, and low power consumption, making it suitable for deployment in various settings such as homes, schools, rural areas, and small industries. Moreover, the modular and scalable architecture allows for the addition of more sensors and communication modules like GSM or GPS to expand the system's capabilities for broader applications. The system's fast response time, minimal false alarms during testing, and consistent reliability under simulated disaster scenarios validate its potential for real-world use. Although it is currently designed for small-scale implementation, the system lays a strong foundation for future advancements in disaster management technology. Features such as cloud integration, mobile app connectivity, data analytics,

and machine learning for predictive alerts can be incorporated to enhance its functionality further. Overall, this work contributes to the growing field of smart disaster response systems and demonstrates how accessible technologies can play a significant role in improving public safety, reducing response time, and building more resilient communities in the face of natural disasters.

References

- [1] R. Kumar, A. Sharma, and M. Singh, "IoT Based Smart Flood Monitoring System Using Ultrasonic Sensor and GSM," *International Journal of Engineering Research & Technology*, vol. 9, no. 6, pp. 1230–1233, 2020.
- [2] S. Patil and S. Kale, "IoT Based Forest Fire Detection System," *International Journal of Innovative Research in Science, Engineering and Technology*, vol. 8, no. 4, pp. 4517–4521, 2019.
- [3] A. R. Al-Ali et al., "IoT-based Smart Disaster Management System for Early Warning," *Future Generation Computer Systems*, vol. 105, pp. 124–134, 2020.
- [4] A. Sharma, P. Mehra, and V. Bansal, "Predictive Analysis for Disaster Management using IoT and Machine Learning," *Procedia Computer Science*, vol. 173, pp. 453–460, 2020.
- [5] T. Ahmad et al., "Challenges and Security Issues in IoT-Based Disaster Management Systems," *Sensors*, vol. 21, no. 8, pp. 1–22, 2021.

**Debabrata Sahoo, Aman Kumar,
Pradeep Kumar Sahoo, Aryan Panda**
Dept. of EEE

Kip Thorne: A Visionary of Modern Physics



Kip Thorne is one of the leading theoretical physicists of our time. His work has deepened our understanding of gravity, black holes, and the fabric of space and time. On June 1, 1940, he was born in Logan, Utah, in the United States. He demonstrated enhanced academic aptitude at a young age. He attended the California Institute of Technology (Caltech) to complete his undergraduate education. After that, under the guidance of John Archibald Wheeler, he earned his Ph.D. at Princeton University. He subsequently became the Feynman Professor of Theoretical Physics after returning to Caltech as a faculty member. His primary areas of study are astrophysics and gravity. One of the key scientists and engineers working on the Laser Interferometer Gravitational-Wave Observatory (LIGO) project was Thorne. It was created to identify gravitational waves, which are space-time ripples. In 1916, Albert Einstein made the first prediction about these waves. But for

almost a century, they went unnoticed. Thorne pushed for scientific advancement to discover them since he believed in their existence. The first gravitational wave detection was made by LIGO in 2015. It was a historic discovery. It validated one of Einstein's main general relativity predictions. Additionally, it signalled the start of a new age in astrophysics. Thorne, Rainer Weiss, and Barry Barish were awarded the 2017 Nobel Prize in Physics. Because of their efforts, gravitational wave astronomy is now a reality.

Kip Thorne is renowned for his endeavours to make science more accessible. He was heavily involved in the production of the 2014 movie *Interstellar*. He was the movie's executive producer and scientific advisor. He made sure the film's scientific material was correct. He came up with two key guidelines for the science in *Interstellar*, and one of them was that nothing in the film would violate established laws of physics — it showed how deeply grounded he was in science. The black hole “Gargantua” in the movie was based on real physics. Thorne's input gave the film scientific import as well as aesthetic beauty. Subsequently, he wrote a book titled ‘The Science of Interstellar’. The book is an explanation of the science behind the film in layman's language. Thorne's interests are not limited to gravitational waves. He has done a lot of writing about time travel, wormholes, and the boundaries of physical law. He thinks the general population should have access to difficult science. Engineers and scientists alike are inspired by his work. His vision keeps pushing the limits of time, space, and human creativity. He remains a remarkable character in modern science.

In a time when science and creativity sometimes clash, Kip Thorne serves as a reminder that when driven by curiosity and the principles of nature, rigorous scientific investigation and imaginative thought may coexist and even flourish.

Sanigdha Samal
4th Sem, Dept. of EE

Customized Electronic Tongue

The novelty of this work lies in the fabrication of a low-cost portable device for proper analysis of food quality. Additionally, the sensing materials are prepared based on the molecularly imprinted polymer (MIP) technique, which has been serving as a promising alternative to the above-mentioned hindrances. MIP is basically a recognition tool that creates vacant sites similar in orientation to the target analyte on the polymer surface. On exposure of the analyte to the polymer matrix, the analyte gets trapped within the cavities of the polymer and thus gets recognized. For the case of tea, out of approximately 500 compounds present, only 5-6 (catechin, theaflavin, EGCG, etc) affect its quality. Therefore, we have planned to detect those five quality-affecting compounds in tea by developing sensors based on the novel MIP technique. Likewise, the quality of milk, fish, turmeric, etc, can be assessed by simply fabricating specific MIP sensors specific for formalin, metanil yellow, hexamine, Ethylenediaminetetraacetic acid (EDTA), Niacin, Saccharin, etc. No such array of MIP electrodes for quality assessment of agro-products has been developed so far. The interesting thing about this portable device is that it can be employed for quality assessment of any food product or beverage, just by replacing the sensors.

The cost of the Potentiostat has been targeted to be reduced by thousands. Fabrication of the compact device and the voltammogram display in the Raspberry Pi module is yet to be done. In the trading industry, food additives are commonly used to promote the products or increase their export worthiness. Nevertheless, these substances can be hazardous or beneficial at different concentrations.

For instance, formalin is used in the preservation of various items like fish, meat, mushrooms, milk, fruits, and vegetables; biological accumulation of formaldehyde, a carcinogenic substance, beyond acceptable intake levels of 0.15 to 0.2 mg/kg/day can be life-threatening.

A common malpractice among traders in India is the use of metanil yellow, an illicit synthetic dye. Metanil yellow is a toxic azo ($N=N$) dye containing the sodium salt of [m-(panilinophenyl) azo] benzene sulfonic acid and has been categorized as a CII substance by the Joint Food and Agriculture Organization of the United Nations/World Health Organization. Consumers' effective consumption may increase their risk of developing tumours, neurotoxicity, hepatocellular carcinoma, lymphocytic leukemia, and other chronic illnesses.

To mitigate health risks associated with metanil yellow in food, strict enforcement of the maximum permissible limit of 100 mg/kg is essential. The impact of other food additives, preservatives, artificial sweeteners, nutritional supplements, acidity, or pH regulators is studied in recently developed research.

Tea is beneficial for human health as it is rich in antioxidants and prevents us from deadly diseases like diabetes mellitus, Alzheimer's, Parkinson's, cancer, etc. Tea can act as a savior only if the consumers intake tea of proper quality.

For effective quality monitoring, investors are developing simple, cost-effective, portable devices with high-end instrument specifications like precision, selectivity, robustness, sensitivity, small power consumption, reproducibility, and measurement time. Customized electrodes that just measure food or beverage quality would provide a more objective analysis. Therefore, it will directly affect food and beverage prices. The industries will also benefit in a way, as they no longer have to use any generalized instrument that can estimate the quality of almost all foodstuffs.

Dr. Debangana Das
Dept. of EE

CRISPR & Bioinformatics: Editing Life with Precision

In the age of rapid technological advancement, the convergence of bio-informatics and gene-editing tools like CRISPR (Clustered Regularly Inter spaced Short Palindromic Repeats) is revolutionizing biology and medicine. While CRISPR brings the capability to modify genetic material with unprecedented accuracy, bio-informatics provides the computational backbone to decode, predict, and optimize these modifications. Together, they are paving the way for a future where inherited diseases may be preventable, therapies more effective, and our understanding of life itself deeply transformed.

The Power of CRISPR: A Genetic Scalpel

CRISPR is often likened to molecular scissors that can cut DNA at precise locations, enabling genetic material removal, addition, or alteration. Originally discovered as a bacterial immune defense mechanism, CRISPR has become a transformative gene-editing platform due to its simplicity, adaptability, and cost-effectiveness.

At its core, CRISPR-Cas9 involves a guide RNA (gRNA) that directs the Cas9 enzyme to a specific DNA sequence. Once there, Cas9 makes a cut, and the cell's natural repair machinery either disrupts or replaces the targeted gene. This ability to rewrite the genetic script has opened doors for applications in treating genetic disorders, enhancing crop resilience, and combating viral infections like HIV.

Where Bioinformatics Enters the Picture

While CRISPR provides the tools to edit DNA, bioinformatics plays the crucial role of identifying where and how to make these edits safely. Genomic data is vast—each human genome comprises over 3 billion base pairs—and finding the right target requires precision that only advanced computational methods can offer.

Bioinformatics algorithms help researchers:

- Analyze genomic sequences to identify potential CRISPR target sites
- Predict off-target effects that might cause unintended gene edits
- Simulate outcomes of gene editing before lab experimentation
- Annotate genes with their functions, locations, and disease associations
- Without bioinformatics, CRISPR's scalpel would be swinging in the dark. With it, editing becomes informed, optimized, and significantly more reliable.

Real-World Impact: From Bench to Bedside

One of the most groundbreaking uses of CRISPR-bioinformatics synergy has been in developing treatments for genetic diseases like sickle cell anemia, beta-thalassemia, and certain forms of blindness. For instance, in clinical trials, scientists have used bioinformatics to map mutations in patient genomes and then employed CRISPR to precisely correct those mutations. Early results have been promising, with some patients showing restored function and improved quality of life.

In agriculture, scientists are using bioinformatics to scan plant genomes for genes associated with drought tolerance or pest resistance. Once identified, CRISPR can be used to tweak those genes, creating hardier, more sustainable crops without introducing foreign DNA—a key concern in traditional GMO approaches.

Ethics, Accuracy, and the Future

As powerful as this technology is, it also raises significant ethical and safety concerns. Editing the germline—heritable DNA in embryos—could alter human evolution if misused. Bioinformatics can act as a safeguard here by rigorously predicting risks, suggesting alternatives, and helping ensure edits are precise and justified.

Moreover, as AI becomes increasingly integrated into bioinformatics, the ability to model entire biological systems before making real-life interventions is within reach. Imagine a future where we can simulate how gene editing might affect not just an individual, but generations to come.

Conclusion: Precision with Purpose

CRISPR and bioinformatics together represent the fusion of biology and computation—two fields that, when united, offer the ability to heal, enhance, and

perhaps one day, even design life itself. But with this power comes responsibility. The next chapter in genetic science will not be written in DNA alone, but in code, algorithms, and informed choices guided by ethics.

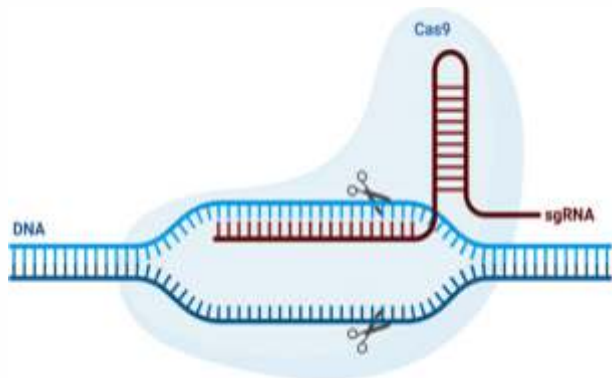


Figure 1. CRISPR-Cas9 gene-editing system

Figure 1 illustrates the CRISPR-Cas9 gene-editing system, a revolutionary biotechnology tool used for precise modifications in DNA. CRISPR/Cas9 technology comprises several essential components that enable precise genome editing. Firstly, the Cas9 protein acts as a molecular scissors and nuclease, capable of cleaving the DNA strands at specific

locations. Secondly, the single guide RNA (sgRNA) serves as a molecular guide, providing Cas9 with the sequence information necessary to target and bind to the desired DNA site. The sgRNA consists of a CRISPR RNA, which recognizes the target sequence, and a trans-activating CRISPR RNA, which aids in Cas9 binding.

Figure 2 depicts CRISPR-Cas9 technology, which is extensively employed in agriculture to improve the characteristics of crops and livestock. It facilitates the development of precision genetic modifications to enhance livestock productivity and generate precise information in live animals for research. In the production of biofuels, CRISPR is instrumental in increasing the yields of lipids in yeast and algae. Additionally, it enhances the quality, resistance, and shelf life of crops such as soybeans, rice, and maize.

The applications of CRISPR-Cas9 technology in the field of medicine are illustrated in Figure 3. It is employed to rectify genetic disorders such as hemophilia, beta-thalassemia, and cystic fibrosis by editing defective DNA. Furthermore, CRISPR facilitates drug development by identifying and screening novel targets for potential therapeutic medicines.

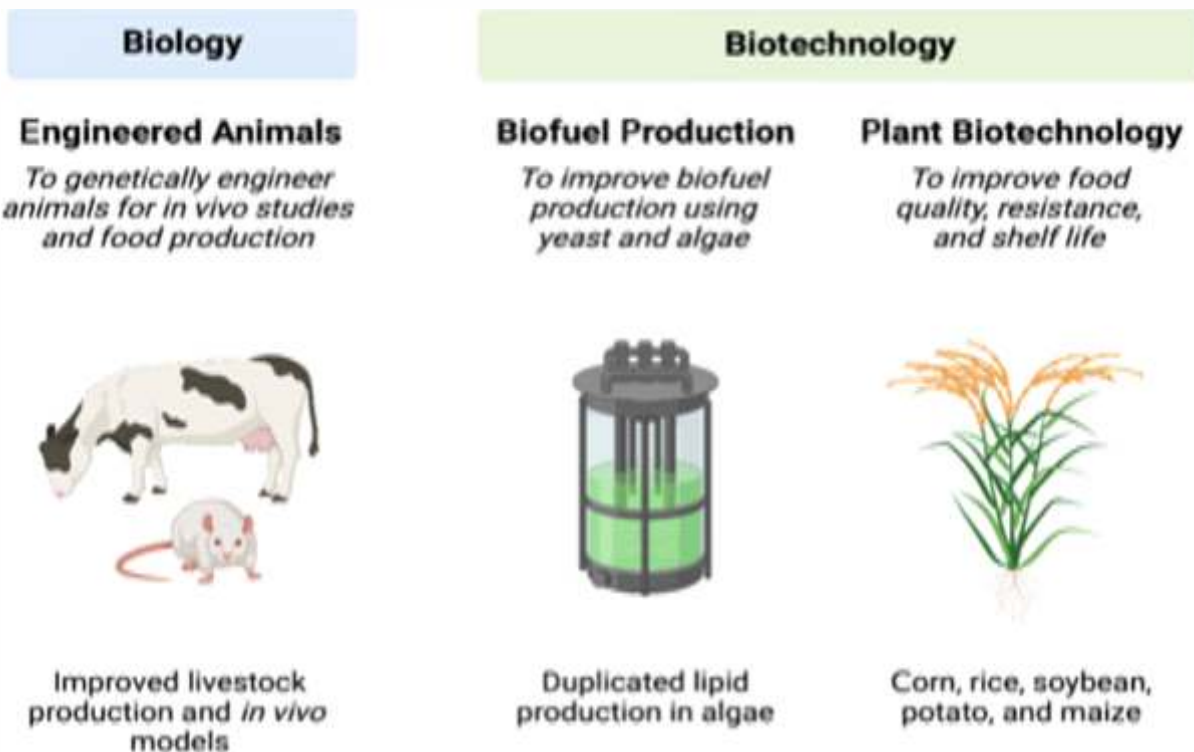


Figure 2. Applications of CRISPR-Cas9 technology for genome editing in the field of agriculture

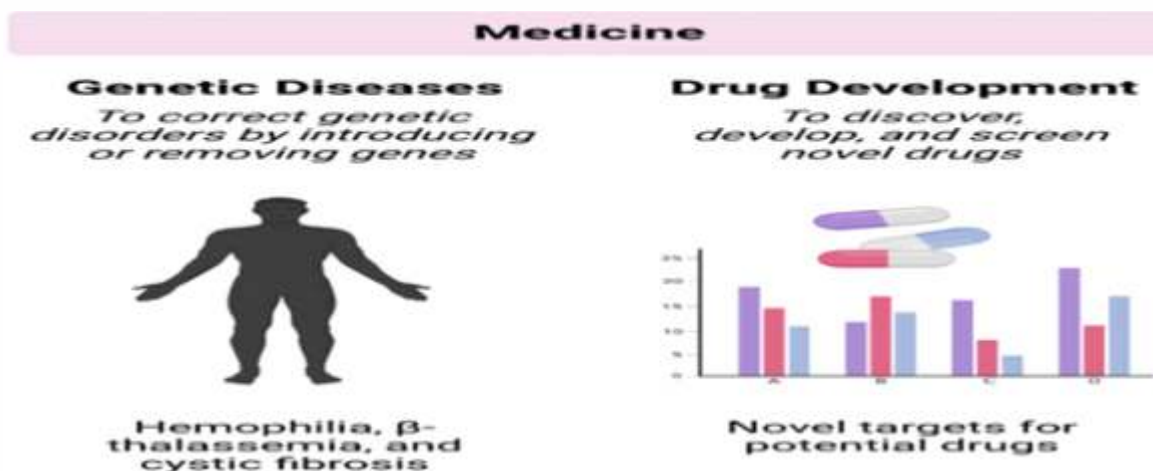


Figure 3. Applications of CRISPR-Cas9 technology for genome editing in the field of medicine

Reference:

- [1] Ansori, A. N., Antonius, Y., Susilo, R. J., Hayaza, S., Kharisma, V. D., Parikesit, A. A., ... & Burkov, P. (2023). Application of CRISPR-Cas9 genome editing technology in various fields: A review. *Narra J*, 3(2), e184.
- [2] Choudhary, S., Ubale, A., Padiya, J., & Mikkilineni, V. (2020). Application of bioinformatics tools in CRISPR/Cas. In *CRISPR/Cas Genome Editing: Strategies And Potential For Crop Improvement* (pp. 31-52). Cham: Springer International Publishing.

Prachi Pratyasha Das
4th Sem, EE

Clever chemistry can make rocks absorb CO₂ much more quickly



Olivine rock naturally reacts with carbon dioxide

Spreading crushed rocks on fields can absorb CO₂ from the air – now chemists have devised a way to turbocharge this process by creating more reactive minerals.

A new process could enable crushed rocks to capture carbon dioxide from the air much more quickly, turbocharging a carbon removal technique that is already being widely adopted.

Natural silicate minerals such as basalt react with water and CO₂ to form solid carbonate materials, a process known as enhanced rock weathering (ERW). Studies suggest that spreading crushed silicate rocks on agricultural land can increase the amount of carbon that soil can absorb while also improving crop yields for farmers.

Source: www.newscientist.com

Plastic Pollution in the Ocean



Courtesy: Vincent Kneefel

Plastic has become ubiquitous in our daily lives because of its convenience and low prices. Our mistreatment and mismanagement of the material have made it one of the biggest environmental problems of our lifetime. Millions of tons of plastic waste are dumped every year, a majority of which makes its way into the oceans, harming wildlife and ecosystems in the process. Yet 91% of all plastic that has ever been made is not recycled. The first commercially available plastic product was launched in 1907, but mass production didn't start until 1952. Since then, annual plastic production has increased nearly 200-fold, where today, we produce as much plastic globally as two-thirds of humanity's total mass. Our reckless plastic use and consumption have driven the world to generate approximately 400 million tonnes of plastic waste each year to keep up with demand, 60% of which ends up in our natural environment or landfills.

More than 8 million tonnes of plastic enter the oceans every year. Ocean plastic pollution is on track to rise to 29 million metric tons by 2040, and 1,00,000 animals die from plastic entanglement each year. COVID-19 has added 25,900 tonnes of plastic pollution to the ocean. According to recent research, this extensive increase in plastic consumption has resulted in an estimated 8.4 million tonnes of plastic waste generated from 193 countries since the start of the pandemic, and 25,900 tonnes of which, equivalent to more than 2,000 double-decker buses, have leaked into the ocean. With negotiations for a global plastic treaty in full swing and it is crucial to take action now to reduce our global plastic consumption and production before it's too late to reverse the damage.

Source: <https://earth.org/plastic-pollution-statistics/>

Design of a Miniaturized Wearable Antenna for Biomedical Applications

Abstract – A significant advancement in wireless communication systems demands low-cost, compact, lightweight, and multi-band antenna structures for efficient signal transmission and reception. The proposed antenna features a cotton substrate, making it highly flexible and suitable for wearable applications. It operates at a resonant frequency of 2.45 GHz, falling within the Industrial, Scientific and Medical (ISM) band, commonly used for wireless communication. A key innovation in this design is the use of two different conducting materials for the top patch and bottom ground plane, which helps optimize performance. To further enhance signal reception is incorporated, improves sensitivity and reduces interference. Essential design considerations include portability, gain, bandwidth, flexibility, and body compatibility for wearable applications. The antenna is designed and optimized using High Frequency Structure Simulation (HFSS) software and will be physically fabricated and validated through experimental measurements to ensure reliability in real-world scenarios.

Keywords – Textile antenna, Wearable Technology, ISM band, Biomedical and defense applications.

I. Introduction

Wearable antennas are specialized antennas designed to be integrated into clothing or worn directly on the body. They are a critical component in modern body-centric wireless communication systems, enabling a wide range of applications such as health monitoring, sports performance tracking, military communications, and wearable IoT devices. These antennas must operate efficiently while maintaining flexibility, comfort, durability, and safety for the user. The most crucial area of research in wearable technology is textile-based antennas. As most people's daily needs include clothing, it leads researchers to integrating electronic devices into their clothes to create smart clothing. Textile or wearable antennas are more suitable for body-centric wireless systems.

The signal/data across the embedded device and the wearable device is received and sent by the wearable antenna; thus, a wearable antenna is a crucial part of our lives. Human beings act as a lossy medium for EMW, so the antenna must be fabricated as effectively as feasible, and these waves are absorbed by the body in the form of heat and energy. This paper proposes a C-shaped slot wearable antenna with jeans as a substrate. The antenna satisfies the unlicensed ISM band 2.45 GHz.

Various techniques of feeding wearable antennas and their literature searches are conducted, and observations include the following:

A keyhole-shaped wearable wideband antenna designed for ISM, WiMAX, and WLAN applications was proposed in [1]. The antenna uses jeans cloth as a flexible, low-cost substrate, with a dielectric constant of 2, making it ideal for integration into clothing. Covering a frequency range from 1.99 to 5.42 GHz, the design achieves a peak realized gain of 2.5 dB at 2.45 GHz and 5.21 dB at 5.42 GHz. The antenna combines a compact size ($50 \times 35 \times 1.59 \text{ mm}^3$) with wideband performance and low SAR, making it suitable for wearable communication systems. Simulation and design were performed using Ansys HFSS software.

A compact wearable textile antenna designed for biomedical applications, operating at the 2.45 GHz ISM band, was proposed in [2]. The antenna uses a cotton substrate for flexibility and employs two different conductive materials: copper tape and silver shieldit. The design shows good reflection coefficients (-31.05 dB for silver and -35.52 dB for copper) and compact dimensions ($60 \times 70 \times 2 \text{ mm}^3$). The study highlights that copper tape offers better gain and efficiency, while silver shieldit provides superior flexibility, making it ideal for wearable health-monitoring systems. Simulation and experimental results confirm the antenna's suitability for wearable biomedical communication.

The paper presents a compact dual-mode, pattern-reconfigurable wearable antenna designed for 2.4 GHz Wireless Body Area Network (WBAN) applications in [3]. The antenna uses TM00 and TM10 modes to

switch between omnidirectional (ON-body) and unidirectional (OFF-body) radiation patterns. A rectangular slot and four p-i-n diodes enable this reconfigurability, allowing mode switching based on the communication scenario. The antenna shows stable performance on different body parts, maintains safety within SAR limits, and demonstrates reliable impedance matching, gain, and radiation patterns. Its design combines a rigid and flexible substrate, making it suitable for wearable devices in healthcare, rescue, and personal communication systems.

The paper proposed in [4] advancements in compact, high-efficiency antennas for wearable devices, particularly for medical and wireless communication applications. Traditional small antennas often suffer from low efficiency, which the study addresses using metamaterials and fractal antenna technologies. Splitting resonators (SRR) integrated into antennas improve gain and reduce resonant frequency by 5–10%. The directivity and gain of SRR-enhanced antennas are higher by approximately 2.5dB compared to standard patch antennas. Fractal antennas, known for their compact and multiband characteristics, exhibit high gain (up to 8dBi) and efficiency (up to 97%). Simulations and measurements were carried out using full-wave 3D modelling tools, showing good agreement between computed and actual results. The designs emphasize dual polarization, reduced size, and adaptability for integration with clothing or medical belts. Overall, this study highlights how innovative antenna structures can enhance performance in wearable systems, especially for healthcare monitoring and wireless data transmission

The paper proposed in [5] introduces a compact multi-slot wearable patch antenna specifically designed for wireless communication applications operating at 6.1 GHz. The antenna uses a cotton substrate, which makes it highly suitable for wearable applications due to its flexibility, comfort, and easy integration with clothing materials such as shirts, belts, and jackets. The proposed antenna features a compact design with dimensions of 42 mm × 32 mm × 3 mm and incorporates 13 rectangular slots to enhance its electrical performance while maintaining a lightweight and low-profile structure. The Voltage Standing Wave Ratio (VSWR) is recorded as low as 1.05, highlighting efficient power transmission. The antenna's peak gain reaches 6.6 dBi, and its radiation pattern exhibits strong directivity with a front-to-back

ratio of 21.4 dB, making it ideal for wearable communication systems.

II. Antenna Design and Structure

The proposed design is a compact wearable microstrip patch antenna optimized for 2.45 GHz ISM applications. Using MATLAB and simulation tools, the antenna integrates circular and rectangular slots for miniaturization, impedance matching, and flexibility. The design ensures stable performance under deformation, making it ideal for health monitoring, WBANs, and IoT wearable devices.

By using the following empirical formulae (1 & 2), the inception design parameters of the proposed Radiating Patch Antenna (RPA) are obtained:

$$R = \frac{F}{\left\{1 + \frac{2h}{\pi \epsilon_r F} \left[\ln \left(\frac{\pi F}{2h} \right) + 1.7726 \right] \right\}^{1/2}} \quad (1)$$

Where

$$F = \frac{8.791 \times 10^9}{f_r \sqrt{\epsilon_r}} \quad (2)$$

R = Patch radius.

h = Substrate height.

f_r = Frequency of resonance of the microstrip patch

ϵ_r = Relative permittivity of the substrate.

The design parameters of the proposed antenna is displayed in Table I. These parameters were optimized using the parametric optimization built into HFSS to obtain the desired results.

Table I. Patch Antenna Dimension

Dimension	Value (mm)
Radius of Patch (RR)	30 mm
Height of the Substrate (h)	1.6 mm
Wavelength (λ ₀)	125 mm
Feed x-coordinate (fx)	4 mm
Feed y-coordinate (fy)	11.42 mm
Radius of inner conductor of coaxial (R1)	0.7 mm
Radius of outer conductor of coaxial (R2)	1.6 mm
X coordinate of the starting point of arc (Ax)	6 mm
Y coordinate of the starting point of arc (Ay)	6 mm
Arc Angle (Aα)	79.5 Degree
Arc Width (Aw)	1 mm
Slot Length	18 mm
Slot Width	3.5 mm
Ground Plane Length (Lg)	50 mm
Ground Plane Width (Wg)	50 mm
Arc Width (Aw)	1 mm
Slot Length	18 mm
Slot Width	3.5 mm
Ground Plane Length (Lg)	50 mm
Ground Plane Width (Wg)	50 mm

A range of techniques is used in the feeding of microstrip patch antennas. For example, proximity coupling feed, microstrip line feed, and aperture coupling are some of them. The suggested antenna uses the microstrip line feeding method. Some of the advantages of this feeding are that it has good impedance matching and is low radiating. The proposed RPA's different aspects are shown in Figure 1.

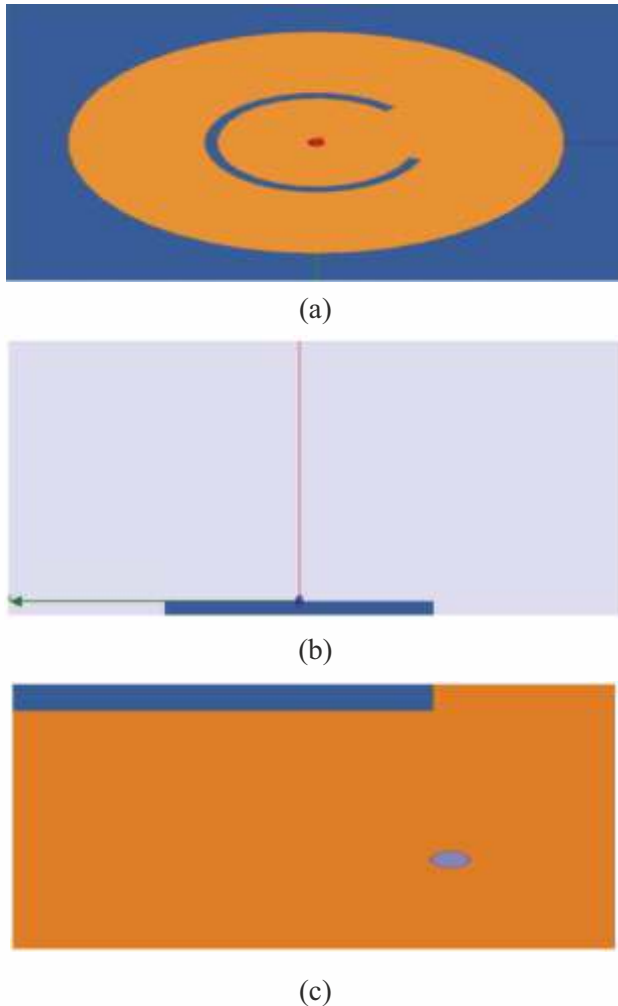


Fig. 1. (a) Top view, (b) Side view, (c) Bottom view of the antenna with line feed

To enhance the gain, a Microstrip line feed is applied to the FR4 Epoxy substrate having a permittivity of 4.4.

II. Results and Discussions

To design and simulate the proposed antenna, we have used ANSYS HFSS software. The designed antenna resonates at 2.45 GHz. The proposed antenna S11

parameter is also good, and they are 16.0698 dB. On the other hand, the proposed antenna sees an impedance of 59.54 and -14.52, respectively; the antenna's S11 feature is shown in Figure 2.

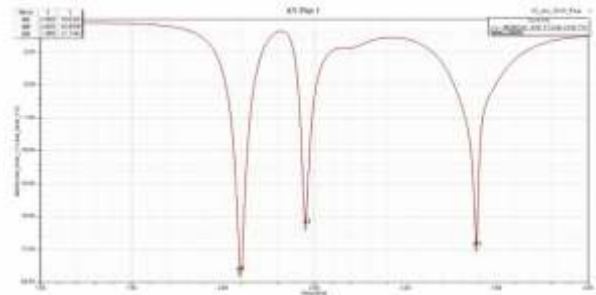


Fig. 2. Return loss S11 (dB) vs Frequency (GHz) of the antenna

The maximal power transfer theorem should be followed in an antenna to be properly matched to the impedance. To excite the designed antenna, 50-ohm feed line impedance is used. The results show that the RPA consists of real parts of 59.54 Ohm and imaginary parts of -14.52 Ohm, for a frequency of 2.45 GHz that resonated respectively.

Good impedance matching of the antenna is determined, facilitating signal transmission. Figures 3 and 4 show the far field radiation pattern at a specified frequency, and as per the plot, the radiation pattern is essentially omnidirectional.

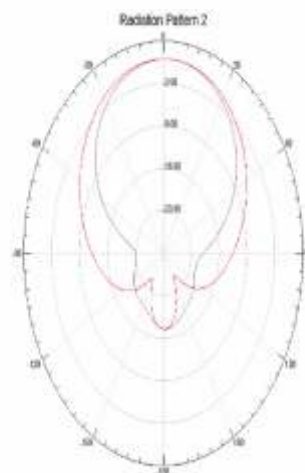


Fig 3. Far Field Radiation Pattern at 2.45 GHz with gain

The antenna exhibits measurable gain at 2.05 GHz, contributing to its overall performance across the operating frequency range.

The Voltage Standing Wave Ratio (VSWR) value should be 1, ideally, and getting almost the ideal value

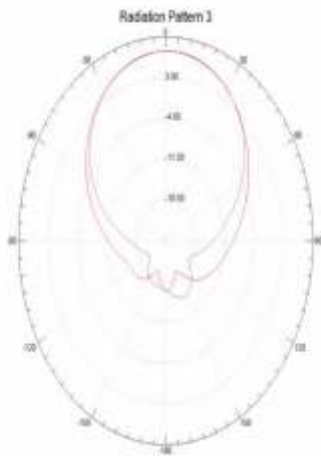


Fig. 4. Far Field Radiation Pattern at 2.45 GHz with gain

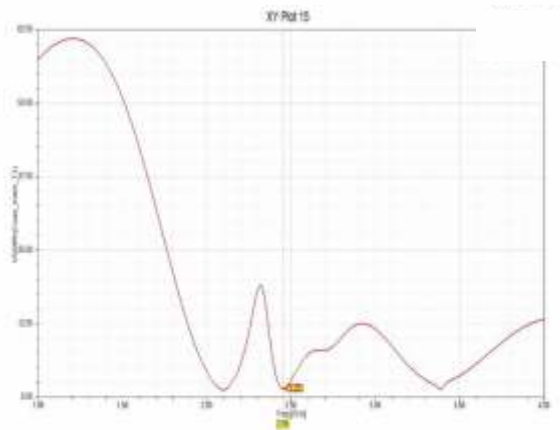


Fig. 5. VSWR characteristics at $f = 2.45$ GHz

is the antenna as 1.37. Thus, signals will be transmitted at their maximum. Figure 5 shows the VSWR characteristic of the RPA.

IV. Conclusion

The miniaturized wearable antenna designed and optimized using HFSS software demonstrates excellent performance for biomedical applications. The antenna is specifically tuned to resonate at 2.45 GHz, a widely used frequency in medical and wireless body area network (WBAN) systems. The achieved VSWR value of 1.37 at the target frequency indicates effective impedance matching, ensuring minimal signal reflection and maximum power transmission. The compact size and optimized design make the

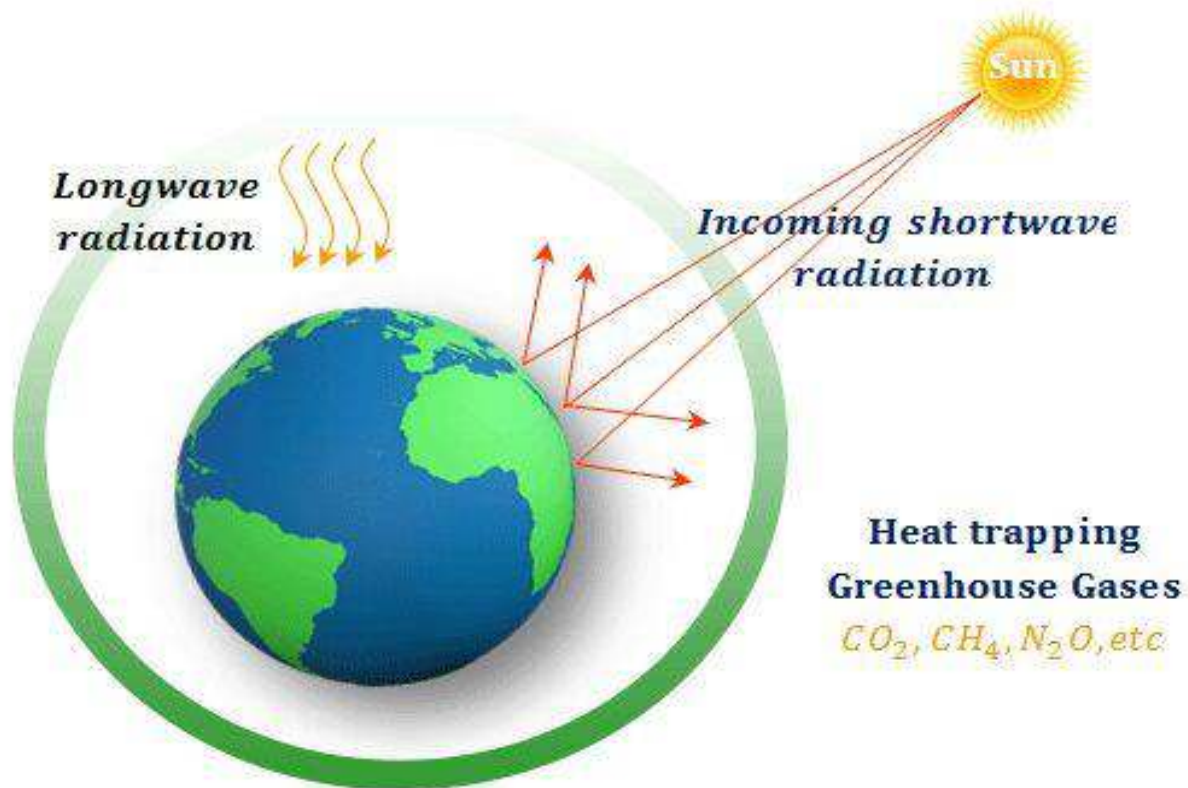
antenna highly suitable for integration into wearable medical devices, offering reliable communication, enhanced comfort, and efficient performance. This design proves promising for future biomedical and health-monitoring applications.

References

- [1] A Keyhole-Shaped Wearable Wideband Antenna with Partial Ground Plane for ISM, WiMAX & WLAN Applications Kumar, Saurabh & Anand, Shivani & Bharti, Gagandeep. (2023). . 1-4. 10.1109/ICICAT57735.2023.10263711.
- [2] S. Shrivastava, A. Bansal and S. Malhotra, "Compact wearable textile antenna design for Biomedical Applications," 2023 First International Conference on Microwave, Antenna and Communication (MAC), Prayagraj, India, 2023, pp. 1-5, doi: 10.1109/MAC58191.2023.10177127.
- [3] G. -P. Gao, B. -K. Zhang, J. -H. Dong, Z. -H. Dou, Z. -Q. Yu and B. Hu, "A Compact Dual-Mode Pattern-Reconfigurable Wearable Antenna for the 2.4-GHz WBAN Application," in IEEE Transactions on Antennas and Propagation, vol. 71, no. 2, pp. 1901-1906, Feb. 2023, doi: 10.1109/TAP.2022.3225529.
- [4] A. Sabban, "Small wearable antennas for wireless communication and medical systems," 2018 IEEE Radio and Wireless Symposium (RWS), Anaheim, CA, USA, 2018, pp. 161-164, doi: 10.1109/RWS.2018.8304974.
- [5] M. S. S. S. Srinivas, A. K. Gupta, B. R. Babu, A. V. S. Swathi, P. S. R. Chowdary and T. V. Ramkrishna, "Multi Slot Wearable Patch Antenna for Wireless Applications," 2024 IEEE Wireless Antenna and Microwave Symposium (WAMS), Visakhapatnam, India, 2024, pp. 1-4, doi: 10.1109/WAMS59642.2024.10527935.

Renuka Singh, Sanchita Kumari, S Debajyoti
Dept. of EE

Greenhouse Effect, Global Warming & Joseph Fourier...



It is a common misconception that the Earth's Greenhouse Effect and Global Warming are the same thing. They are not. The discovery that the Earth has a Greenhouse Effect is generally attributed to the French Scientist Jean-Baptiste Joseph Fourier, although he did not explicitly use that phrase. As early as 1824, Fourier theorized that an object the size of the Earth, and at its distance from the Sun, should be considerably colder than the planet is, if only warmed by solar radiation. He realized that the Earth's atmosphere has gases like carbon dioxide and water vapor which trap the longer wavelengths of solar radiation, heating it and allowing lifeforms as we know of to exist. Without the Greenhouse Effect, the average temperature of the Earth's surface would be a bone-chilling $-18^{\circ}C$!

The term Greenhouse Effect first appeared in the work of Swedish meteorologist Nils Gustaf Ekholm around 1900.

Now, coming to Global Warming. It is an enhancement of the Greenhouse Effect, where human activities, primarily the burning of fossil fuels, have increased concentrations of CO_2 , resulting in significant warming of the atmosphere. There is now widespread concern that the resulting increased atmospheric temperature will have catastrophic consequences if it is not arrested or reversed.

(Content excerpted from web sources, including Wikipedia)

Dr. Jaideep Talukdar
Dept. of BSH

Publication Cell

Tel: 9937289499/8260333609

Email: publication@silicon.ac.in

www.silicon.ac.in

The Science & Technology Magazine

Digital Digest



Silicon University, Odisha

Contents

Editorial	2
Special Feature	3
Technology Updates	11
DD Feature	13
Profile of a Scientist	17
PhD Synopsis	18
Breakthrough in Bio-informatics	19
Environmental Concerns	22
Historical Tidbits	27

Editorial Team

Dr. Jaideep Talukdar
Dr. Pragyan Paramita Das
Dr. Lopamudra Mitra

Members

Dr. Nalini Singh
Dr. Priyanka Kar
Dr. Amiya Bhusan Sahoo
Dr. Chittaranjan Mohapatra
Mr. Subrat Kumar Sahu

Student Members

Sanigdha Samal
Prachi Pratyasha Das

Media Services

G. Madhusudan

Circulation

Sujit Kumar Jena

Make your submissions to:
publication@silicon.ac.in